



# Doppler Correction in Moving Narrowband Ultrasonic Ranging Sensors for Small-Scale Motion Tracking

Karalikkadan Ashhar<sup>1</sup> , Mohammad Omar Khyam<sup>2</sup>, Md Noor-A-Rahim<sup>3</sup> , Aruna Jayasuriya<sup>2</sup>, and Soh Cheong Boon<sup>1</sup>

<sup>1</sup>School of Electrical and Electronic Engineering, Nanyang Technological University, Singapore 639798

<sup>2</sup>Department of Electrical Engineering, CQ University, Norman Gardens, QLD 4701, Australia

<sup>3</sup>School of Computer Science and IT, University College Cork, Cork T12 YN60, Ireland

\*Senior Member, IEEE

Manuscript received August 5, 2020; accepted August 14, 2020. Date of publication August 18, 2020; date of current version September 10, 2020.

**Abstract**—Narrowband ultrasonic sensors can be used for motion tracking and small-scale localization. Moving sensor nodes emitting ultrasonic waves produce a Doppler shift in the received signals. Doppler correction methods in narrowband ultrasonic motion tracking systems are explained in this letter. Two methods are suggested for Doppler compensation for small-scale localization using ultrasonic sensors. One of the methods requires a pilot carrier to be added to the transmitted signal and the other method exploits range-Doppler coupling for Doppler correction. In the simulation experiments, we compare the performance of the two methods with the traditional methods. We implement both the methods on hardware and compare the performance of the methods for ranging and localization in the presence of Doppler shift.

**Index Terms**—Sensor networks, chirp compression, correlation receiver, Doppler correction, narrowband ultrasonic sensors.

## I. INTRODUCTION

Narrowband ultrasonic sensors can be used as wearable sensors for motion tracking and gait analysis as they require lower voltages and are cheaper compared to broadband ultrasonic sensors [1], [2]. In narrowband ultrasonic transducers, Doppler correction, multipath compensation, and multiple access for accurately tracking multiple moving markers require various signal processing techniques to be implemented with the limited bandwidth of the sensors. Wideband ultrasonic transducers increase the cost and power requirement of the systems [3]. In this letter, we are considering narrowband piezoelectric transducers having a bandwidth of around 10 kHz. The distance travelled by the transmitted wave can be estimated from time of flight by multiplying by the velocity of the wave. Some of the methods to find the time of flight are thresholding, cross correlation, and phase correlation [4]. The cross-correlation-based method is robust in noisy environments [5]. In the phase correlation method, the maximum measurable range is limited to one wavelength [6]. The maximum measurable range can be improved by combining the phase correlation method with cross-correlation method [6]; however, this method fails when the noise increases. A threshold-based phase-correlation method can be used with narrow bandwidth [7]; however, this method can fail if the signal to noise ratio (SNR) is low or in the presence of multiple access noise. Linear modulated chirp signals can be used to improve the robustness of cross correlation [8]. Chirp signal modulation also enables channel multiple access.

In this letter, we discuss two Doppler correction methods: 1) Pilot-carrier based method and 2) Range-Doppler coupling neutralization method) in correlation receivers with chirp signals in narrowband ultrasonic sensors and compare the performance in terms of tracking accuracy, complexity, and data update rate. The first method is an

adaptation of pilot-carrier method employed in [9] for orthogonal frequency-division multiplexing (OFDM) signals to chirp signals. The second method is adapted from [1] and [3], and we improve the data update rate of the method. Moving sensor nodes emitting ultrasonic waves introduce Doppler shift in the frequency of the received signals. Classical methods for Doppler correction include a bank of correlators [10], [11] and are computationally complex as we need to perform multiple correlations to obtain one measurement update. We propose two improved methods with lower computational overheads for Doppler correction, evaluate the performance, and compare it with existing methods. Chirp signals were found to provide better performance with correlation receivers compared to other coding techniques in terms of Doppler tolerance and peak to average power ratio (PAPR) [2]. PAPR is defined as the ratio of peak value to the RMS value of signal power. OFDM was used for narrowband ultrasonic ranging in [9]. However, it suffers from high PAPR [12]. In ranging systems, it is important to increase the energy and reduce the amplitude peak of the transmitted signal [12]. The PAPR reduction methods depends on signal duration [2]. The performance of OFDM chirp signals and the linear chirp signals are studied in [1] and the linear up-and down chirp signals were found to perform well for two mobile nodes. Hence, we are using linear chirp signals in the proposed methods.

## II. DOPPLER CORRECTION METHODS

Let  $\hat{S}(t)$  be the Doppler shifted version of the originally transmitted signal  $S(t)$ . The received signal  $R(t)$  is given by:  $R(t) = \hat{S}(t) * I(t) + n(t)$ , where  $I(t)$  is the channel impulse response, and  $n(t)$  is the channel noise. At the receiver, correlation output can be given by

$$C(t) = [\hat{S}(t) * I(t) + n(t)] \star S(t). \quad (1)$$

The correlation output at the receiver side provides higher peak amplitude and lower peak width when the correlation operation is performed with the same signal as the received signal. We aim to

Corresponding author: Karalikkadan Ashhar. (e-mail: ashhar001@e.ntu.edu.sg).  
Associate Editor: S.-R. Kothapalli.  
Digital Object Identifier 10.1109/LENS.2020.3017649

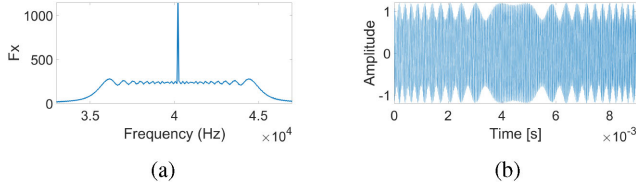


Fig. 1. (a) Frequency response (Fx) of the signal after adding the pilot-carrier. (b) The corresponding signal in time-domain.

reduce the difference between  $\hat{S}(t)$  and  $S(t)$  during correlation. If we can estimate the exact amount of Doppler shift, we can correct the template waveform stored at the receiver side to match the received signal. In the experiments, we used a linear chirp from 35 to 45 kHz of duration 9 ms ( $f_s = 35$  kHz,  $f_e = 45$  kHz, and  $T_s = 9$  ms).

### A. Pilot-Carrier Based Doppler Correction

A computationally efficient Doppler shift estimation using OFDM signal for moving mobile node was proposed in [9]. One of the frequency components was chosen as the pilot carrier, and the amplitude of this particular frequency component was increased compared to other components. However, OFDM signals suffer from high PAPR values [13], [14], and hence we implement a similar pilot carrier based Doppler correction using chirp signals. The method of pilot-carrier generation and Doppler velocity estimation method is explained here: Consider, we took  $2 \times N$  point discrete Fourier transform of  $S(t)$  to get higher resolution in the frequency domain, where  $N$  is the number of samples in the signal sampled at  $F_s$  ( $F_s = 500$  k/125 k samples/s for ranging/localization experiments). We selected the frequency component corresponding to 40 kHz as the pilot carrier as the resonance frequency of the sensors used is 40 kHz and it can provide maximum power for transmission. This frequency component was amplified to five times its normal amplitude. Fig. 1 shows the frequency response of the signal to be transmitted and the corresponding time domain representation. It can be observed that the introduction of pilot-carrier introduces ripples in the envelope of the time-domain signal and thus slightly increasing the PAPR values. Let  $S(t)$  be the chirp signal before amplifying the pilot-carrier. The signal  $S(t)$  in frequency domain can be represented as

$$S(k) = \sum_{t=1}^{2N} S(t) e^{-\frac{2\pi t(k-1)}{2N}} \\ = S(1) + S(2) + \dots + S(k_p) + \dots + S(2N) \quad (2)$$

where  $k_p$  is the pilot frequency component. We modify the amplitude of the pilot-carrier by multiplying its amplitude by  $A_p$  to get  $\hat{S}(k)$

$$\hat{S}(k) = S(1) + S(2) + \dots + A_p \times S(k_p) + \dots + S(2N). \quad (3)$$

The time-domain signal after amplifying pilot-carrier can be obtained by taking inverse Fourier transform of  $\hat{S}(k)$

$$\hat{S}(t) = \frac{1}{2N} \sum_{k=1}^{2N} \hat{S}(k) e^{\frac{2\pi t(k-1)}{2N}}. \quad (4)$$

At the receiver side, the estimated frequency shift is converted to the Doppler velocity of the target using

$$v_d(t) = \frac{-c \times \delta f(t)}{f_p + \delta f(t)} \quad (5)$$

where velocity away from the fixed anchor node is taken as positive,  $\delta f(t)$  is the frequency shift at time  $t$ ,  $f_p$  is the pilot carrier frequency,

which is 40 kHz in this case, and  $c$  is the velocity of sound wave. The estimated Doppler velocity was used for correction of the template waveform at the receiver side using

$$\hat{S}(t) = \cos \left\{ 2\pi \left( b(t) f_s t + \frac{b(t)^2 (f_e - f_s) t^2}{2 \times T_s} \right) \right\} \quad (6)$$

where  $b(t) = \frac{v}{(v+v_d(t-T_s))}$  and  $0 \leq t \leq \frac{T_s}{b(t)}$ . One ranging cycle, in this case, spans 20 ms. To avoid large errors, the Doppler velocity was set zero if the estimated Doppler velocity lies outside the range of  $V_{dmin}$  to  $V_{dmax}$ , which was set to  $-4$  to  $4$  m/s.

### B. Range-Doppler Coupling Neutralization Method

Ranging using linear chirp signals introduces an error in the measured value, which is proportional to the velocity of moving target known as range-Doppler coupling [15]. In this case, the range-Doppler coupling property of the linear chirp signals is utilized for Doppler velocity estimation. The range-Doppler coupling error will be positive or negative depending on the chirp direction. Consider the up and down-chirp signals given as follows:

$$S_u(t) = \cos \left\{ 2\pi \left( f_s t + \frac{(f_e - f_s) t^2}{2 \times T_s} \right) \right\} \quad 0 \leq t \leq T_s \\ S_d(t) = \cos \left\{ 2\pi \left( f_e t - \frac{(f_e - f_s) t^2}{2 \times T_s} \right) \right\} \quad 0 \leq t \leq T_s \quad (7)$$

where  $f_s$  and  $f_e$  represent the starting and the ending frequencies, which were set as 35 and 45 kHz, respectively.

The estimated range using up- and down- chirp signals can be given as follows:

$$l_1(t) = l_0(t) + \frac{\dot{l}(t) f_0 T_s}{B}, \quad \text{for up-chirp} \\ l_2(t) = l_0(t) - \frac{\dot{l}(t) f_0 T_s}{B}, \quad \text{for down-chirp} \quad (8)$$

where  $l_0$  is the actual range to be estimated,  $l_1$  and  $l_2$  are the range estimated using up- and down-chirp signals, respectively, and  $\dot{l}$  represents the Doppler velocity of the target.  $f_0$  is the center frequency,  $T_s$  represents the signal duration and  $B$  is the bandwidth of the transmitted chirp signal. In each ranging cycle, the estimated Doppler velocity used to correct the waveform for correlation at the receiver side. The differential Doppler-velocity,  $\Delta \dot{l}(t)$  can be calculated by subtracting  $l_2(t)$  from  $l_1(t)$

$$\Delta \dot{l}(t) = [l_1(t) - l_2(t)] \frac{B}{2 f_0 T_s}. \quad (9)$$

At any point,  $t = l_s$ , if the estimated Doppler-velocity is above the maximum set Doppler-velocity,  $V_{dmax}$  or below the minimum set Doppler-velocity,  $V_{dmin}$ , the Doppler-velocity used for correction in the next step is reset to zero. The template signals for correlation at the receiver are corrected to account for the Doppler effect with the Doppler velocities obtained in previous step. The new chirp signals are generated using [16]

$$\hat{S}_u(t) = \cos \left\{ 2\pi \left( b(t) f_s t + \frac{b(t)^2 (f_e - f_s) t^2}{2 \times T_s} \right) \right\} \\ \hat{S}_d(t) = \cos \left\{ 2\pi \left( b(t) f_e t - \frac{b(t)^2 (f_e - f_s) t^2}{2 \times T_s} \right) \right\} \quad (10)$$

where  $b(t) = \frac{v}{(v+v_d(t-T_s))}$  and  $0 \leq t \leq \frac{T_s}{b(t)}$ . The velocity of sound waves given by  $v = 331.5 + 0.6 \times \text{Temperature}$ , and  $v_d(t - T_s)$  is

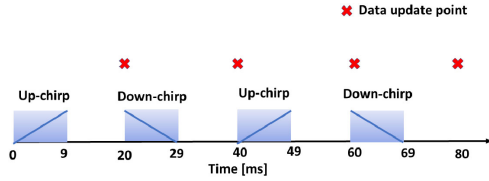


Fig. 2. Representation of data update points in the system.

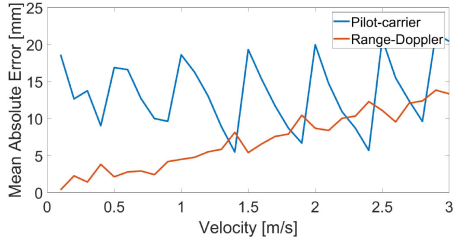


Fig. 3. Effect of Doppler velocities on the two methods.

the estimated Doppler-velocity at time  $t - T_s$  given as follows:

$$v_d(t - T_s) = \sum_{i=0/r_s}^{t-T_s} \Delta \dot{i}(i) \quad (11)$$

In this method, earlier implementations were having the limitation of reduced sampling rate as the samples will be updated in every 40 ms [1], where each transmission of up-chirp and down-chirp takes up 20 ms time. Here, we add additional sample point between the ranging cycles by considering the alternate chirps from consecutive ranging cycles. The data update rate will be maintained at 50 Hz using this method, which is explained in Fig. 2.

The maximum data update rate with narrowband sensors are limited as we need some time between chirp pulses so that the previous pulse or its echoes are died out before a new transmission. Using 50 Hz update rate, we can provide a 11 ms time-gap between 9 ms chirp pulses.

### III. SIMULATION RESULTS

To find the best amplification factor and to study the performance of the proposed methods, we simulated a custom ultrasonic ranging environment in MATLAB. We considered four passive anchor nodes with known positions and one active mobile node. The four anchor nodes were placed at the corners of a  $1 \times 1$  m square. Pilot-carrier at 40 kHz was added to the chirp signal from 35 to 45 kHz and 9 ms duration as explained in Section II-A. The signal was transmitted from the mobile node and received at all the four receivers. We subjected the channel to Gaussian Noise with SNR 0 dB and a multipath component at random positions each time with reflection coefficient 0.4. We avoided close multipath components in the simulations by keeping a minimum separation between the line of sight (LOS) and non-line of sight (NLOS) components equal to  $\frac{1}{B}$  s. The propagation of the ultrasonic signal in the air was modeled as  $A = A_0 e^{-\gamma \times d}$ , where  $A$ ,  $A_0$ , and  $d$  are the amplitude after attenuation, the originally transmitted amplitude, and the distance from transmitter, respectively. We set the attenuation constant  $\gamma$  to 0.17 N·p/m. Initially, we studied the performance of both the proposed methods with varying Doppler velocities. We considered one transmitter moving with respect to one stationary receiver. The simulated Doppler velocity in the transmitted signal was varied from 0 to 3 m/s in steps of 0.1 m/s, and the mean absolute error (MAE) obtained by using both methods are plotted in Fig. 3. Here, we repeated the experiment 100 times and the mean value of MAE was considered. The simulation experiments were also conducted by

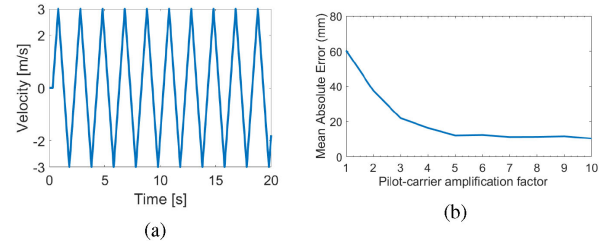


Fig. 4. (a) Simulated velocity of the mobile node. (b) Variation of MAE with pilot-carrier amplification factor.

TABLE 1. MAE Between the Estimated and Actual Range Measurements in Millimeters for Four Different Cases During Simulation Experiments.

Anchor No.	Pilot-carrier	Range-Doppler coupling neutralization	Without Doppler correction	Bank of correlators
1	12.54	0.65	60.3	45.05
2	12.49	0.72	60.27	45.15
3	12.5	0.69	60.27	44.99
4	12.53	0.64	60.29	45.15

moving the mobile node to and fro from the receiver plane with linearly increasing and decreasing velocities between -3 and +3 m/s as shown in Fig. 4(a). The MAE between the estimated distance and the actual distance between the mobile node and each of the anchor nodes was calculated at various pilot-carrier amplification factors. Fig. 4(b) shows the variation of MAE with the pilot-carrier amplification factor. We can observe the mis-identification of the pilot carrier in the received signal caused large errors when the amplification was less than five. Hence, we selected the amplitude of pilot carrier as five times its original value in the rest of the experiments. We used the same simulation environment for ranging using range-Doppler coupling neutralization method, as explained in Section II-B. To compare the performance of the proposed method with existing methods of Doppler correction, we considered simulations in four different scenarios: 1) Pilot-carrier based Doppler correction with amplification factor five, 2) Doppler correction using range-Doppler coupling neutralization method, 3) Ranging without Doppler correction, 4) and a bank of 40 correlation receivers [16].

For the bank of correlators, consider a chirp with  $f_s = 35$  kHz,  $T_s = 9$  ms and  $f_c$  is varied from 43–47 kHz in steps of 100 Hz as explained in [16]. MAE obtained from all the four methods are listed in Table 1. It can be observed that the computationally complex bank of correlators were able to compensate only about 25% of the Doppler errors. The range-Doppler coupling neutralization method gave the best performance. Pilot-carrier based method was able to correct more than 75% of the errors. We repeated the simulation experiments with -5 and -10 dB SNR. The mean value of MAE obtained with 0, -5, and -10 dB SNR are 0.68, 0.84, and 1.04 mm, respectively, for range-Doppler and 12.51, 14.68, and 21.54 mm, respectively, for the pilot carrier based method.

### IV. PENDULUM EXPERIMENTS

A pendulum experiment was designed to test the simulation results and observations with Murata MA40S4S/R ultrasonic transducers as pendulum models are often used to model gait [17]. Initially, experiments were conducted for ranging between one anchor node and one mobile node attached to the pendulum. The pendulum was made to swing almost perpendicular to the receiver plane ( $Y$ -axis). For each trial, the pendulum was released from approximately  $45^\circ$  to the

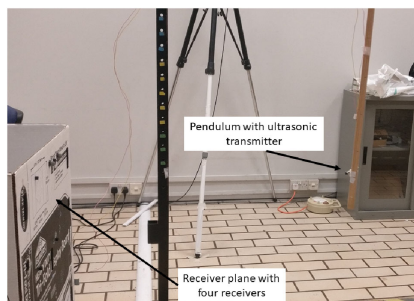


Fig. 5. Setup for pendulum experiment.

TABLE 2. Mean Value of MAE and RMSE During Ranging Experiments.

	Pilot-carrier	Range-Doppler coupling neutralization	Without Doppler Correction
MAE	8.06	3.83	16.93
RMSE	12.29	4.58	20.97

TABLE 3. Mean Value of MAE and RMSE Calculated During Localization Experiments.

	Pilot-carrier	Range-Doppler coupling neutralization	Without Doppler Correction
MAEx	15.79	5.05	9.05
MAEy	6.31	4.90	24.22
MAEz	12.47	8.17	10.21
RMSEx	19.62	7.01	11.59
RMSEy	8.34	6.19	29.82
RMSEz	17.21	10.55	13.74
net-RMSE	27.43	14.19	34.89

vertical direction. The transmitters and the receiver were connected to NI-USB 6343 data acquisition (DAQ) board, which was connected to the PC through USB for postprocessing. The DAQ board drove ultrasonic transmitters by  $\pm 10$  V peak-peak voltage. Optical motion capture system with six high-speed cameras and reflective markers was used as the reference system as explained in [1]. To evaluate the tracking performance, four anchor nodes were used to localize one mobile node attached to the pendulum. The experimental setup is shown in the Fig. 5. An Unscented Kalman Filter [18] was designed to get the 3-D coordinates from the estimated range values.

## V. RESULTS AND DISCUSSIONS

The MAE and root mean square error (RMSE) were calculated from ten ranging experiments each for the proposed methods, and the mean values are listed in Table 2. We calculated  $\text{net-RMSE} = \sqrt{\text{RMSE}_x^2 + \text{RMSE}_y^2 + \text{RMSE}_z^2}$ . It can be observed that the range-Doppler coupling neutralization method gives a higher performance. Pilot-carrier was found to provide satisfactory accuracy.

The MAE and RMSE were calculated from ten localization experiments each for the two methods and without Doppler correction. The mean values are listed in Table 3. Using the pilot carrier method, the error along  $Y$ -direction was found to be much lesser compared to localization without Doppler correction; however, the error along  $X$  and  $Z$  directions increased slightly. The increased error along  $X$  and  $Z$  directions is due to the poor Doppler-frequency resolution in the pilot-carrier based method, which results in some granular noise in the measured range values. If we take 5000-point DFT, the frequency resolution will be 25 Hz and which means that there will be an error of  $\pm 25$  Hz in the detected Doppler frequency, which can translate to an error of  $\pm 7$  mm in the Doppler correction process. This error mainly affects  $X$  and  $Z$  directions during the positioning phase due to the dilution of precision as the anchor nodes are arranged in a plane. The

net-RMSE was found to be better for ranging using the pilot carrier compared with the case without Doppler correction. Compared to other methods using OFDM based chirp signals [9], [14], linear chirp signals are not affected much by higher PAPR values.

## VI. CONCLUSION

To conclude, the range-Doppler coupling neutralization method provided better performance in Doppler correction in moving narrowband ultrasonic sensors compared to pilot-carrier based method. Pilot-carrier based method is computationally less complex compared to the bank of correlators and requires only one correlation per data sample for simultaneous Doppler correction and range measurement. We can obtain the same update rate as the case with ranging using chirp signal without Doppler correction in both the methods as the introduction of Doppler correction does not affect the update rate. This letter focuses on Doppler shift correction methods in narrowband ultrasonic sensors in a single access environment.

## REFERENCES

- [1] K. Ashhar, M. Khyam, C. Soh, and K. Kong, "A Doppler-tolerant ultrasonic multiple access localization system for human gait analysis," *Sensors*, vol. 18, no. 8, 2018, Art. no. 2447.
- [2] M. Khyam, L. Xinde, S. S. Ge, and M. R. Pickering, "Multiple access chirp-based ultrasonic positioning," *IEEE Trans. Instrum. Meas.*, vol. 66, no. 12, pp. 3126–3137, Dec. 2017.
- [3] K. Ashhar, M. Noor-A-Rahim, M. O. Khyam, and C. B. Soh, "A narrowband ultrasonic ranging method for multiple moving sensor nodes," *IEEE Sensors J.*, vol. 19, no. 15, pp. 6289–6297, Aug. 2019.
- [4] M. O. Khyam, S. S. Ge, X. Li, and M. R. Pickering, "Highly accurate time-of-flight measurement technique based on phase-correlation for ultrasonic ranging," *IEEE Sensors J.*, vol. 17, no. 2, pp. 434–443, Jan. 2016.
- [5] R. Queiros, F. C. Alegria, P. S. Girao, and A. C. Serra, "Cross-correlation and sine-fitting techniques for high-resolution ultrasonic ranging," *IEEE Trans. Instrum. Meas.*, vol. 59, no. 12, pp. 3227–3236, Dec. 2010.
- [6] S. Huang, C. Huang, K. Huang, and M.-S. Young, "A high accuracy ultrasonic distance measurement system using binary frequency shift-keyed signal and phase detection," *Rev. Scientific Instrum.*, vol. 73, no. 10, pp. 3671–3677, 2002.
- [7] M. O. Khyam, S. S. Ge, X. Li, and M. R. Pickering, "Highly accurate time-of-flight measurement technique based on phase-correlation for ultrasonic ranging," *IEEE Sensors J.*, vol. 17, no. 2, pp. 434–443, Jan. 2017.
- [8] M. O. Khyam, S. S. Ge, X. Li, and M. R. Pickering, "Pseudo-orthogonal chirp-based multiple ultrasonic transducer positioning," *IEEE Sensors J.*, vol. 17, no. 12, pp. 3832–3843, Jun. 2017.
- [9] M. O. Khyam, S. S. Ge, L. Xinde, and M. Pickering, "Mobile ultrasonic transducer positioning," *J. Eng.*, vol. 2017, no. 4, pp. 119–122, 2017.
- [10] P. Misra, N. Kottege, B. Kusy, D. Ostry, and S. Jha, "Acoustical ranging techniques in embedded wireless sensor networked devices," *ACM Trans. Sensor Netw.*, vol. 10, no. 1, 2013, Art. no. 15.
- [11] F. J. Álvarez, Á. Hernández, J. A. Moreno, M. C. Pérez, J. Ureña, and C. De Marziani, "Doppler-tolerant receiver for an ultrasonic LPS based on Kasami sequences," *Sens. Actuators A, Phys.*, vol. 189, pp. 238–253, 2013.
- [12] R. F. Albuquerque, J. Vieira, I. Lopes, C. A. Bastos, and P. Ferreira, "OFDM pulse design with low PAPR for ultrasonic location and positioning systems," in *Proc. Int. Conf. Indoor Positioning Indoor Navigat.*, 2013, pp. 1–2.
- [13] S. H. Han and J. H. Lee, "PAPR reduction of OFDM signals using a reduced complexity PTS technique," *IEEE Signal Process. Lett.*, vol. 11, no. 11, pp. 887–890, Nov. 2004.
- [14] M. Khyam, S. Ge, X. Li, and M. Pickering, "Orthogonal chirp-based ultrasonic positioning," *Sensors*, vol. 17, no. 5, 2017, Art. no. 976.
- [15] R. J. Fitzgerald, "Effects of range-doppler coupling on chirp radar tracking accuracy," *IEEE Trans. Aerosp. Electron. Syst.*, vol. AES-10, no. 4, pp. 528–532, Jul. 1974.
- [16] P. Misra, "Acoustical localization techniques in embedded wireless sensor networked devices," Ph.D. dissertation, Comput. Sci. & Eng., Fac. Eng., Univ. New South Wales, Sydney, NSW, Australia, 2012.
- [17] A. Salarian, P. R. Burkhard, F. J. Vingerhoets, B. M. Jolles, and K. Aminian, "A novel approach to reducing number of sensing units for wearable gait analysis systems," *IEEE Trans. Biomed. Eng.*, vol. 60, no. 1, pp. 72–77, Jan. 2012.
- [18] S. J. Julier and J. K. Uhlmann, "New extension of the Kalman filter to nonlinear systems," in *Proc. AeroSense*, 1997, pp. 182–193.